Published in : Journal of the American Oil Chemists' Society (2024), vol. 101, n°1, pp. 67–78
DOI: https://doi.org/10.1002/aocs.12781
Status : Postprint (Author's version)

THERMAL AND STRUCTURAL BEHAVIOR OF MANGO (*MANGIFERA INDICA L*) KERNEL FAT FROM THREE IVORIAN VARIETIES

Alfred Kouakou Kouassi[1], Taofic Alabi[2,3], Giorgia Purcaro[4], Erica Moret[5], Christophe Blecker[1], Sabine Danthine[1]

[1] *Food Science and Formulation, University of Liège-Gembloux Agro-Bio Tech, Gembloux, Belgium*
[2] *Department of Animal Biology, University Peleforo Gon Coulybaly, Korhogo, Ivory Coast*
[3] *Functional and Evolutionary Entomology, University of Liège-Gembloux Agro-Bio Tech, Gembloux, Belgium*
[4] *Analytical Chemistry, University of Liège-Gembloux Agro-Bio Tech, Gembloux, Belgium*
[5] *Agri-Food, Environment and Animal Sciences, University of Udine, Udine, Italy*

KEYWORDS

DSC stop-and-return, isothermal crystallization, mango kernel fat, morphology, polymorphism, thermal behavior

ABSTRACT

Mango (*Mangifera indica L.*) seeds is an interesting source of fat, rich in stearic (St) and oleic (O) acid with three major triacylglycerols (TAG): StOSt, StOO, and StLSt. The kernel fat content and quality depend however on the varieties and their origin. The objective of this study was to investigate the crystallization and polymorphic behavior of mango kernel fat extracted from three selected Ivorian varieties which differ in terms of TAG composition: Kent (KT), Djakoumankoun (DN) and Brooks (BR). The isothermal crystallization behavior was examined at 15 and 20°C by pulsed nuclear magnetic resonance, differential scanning calorimetry, x-ray diffraction (XRD) and polarized light microscope. Under static conditions, DN crystallized faster, followed by BR, then KT. At 15°C, an unusual evolution was observed for both DN and BR, which can be explained by a melt-mediated polymorphic transition from α into more stable forms. Using a differential scanning calorimetry (DSC) stop-and-return technique, different crystallization behaviors were also observed. Isothermal XRD experiments confirmed that the kinetics of the polymorphic transformation was different within the three samples, even if the three fats were β-3L-tending. At 15°C, KT transformed from liquid state to stable form without passing through α-form, while DN and BR crystallized first into α-from which transformed further to β', then into stable β-form. At 20°C, DN and BR crystallized directly from liquid to β', which later transformed into β-form while KT did not crystallize under the same conditions. The huge differences observed result from the differences in the TAG profiles, mainly in the StOO and StOSt content.

Published in : Journal of the American Oil Chemists' Society (2024), vol. 101, n°1, pp. 67–78
DOI: https://doi.org/10.1002/aocs.12781
Status : Postprint (Author's version)

Introduction

Crystallization behavior is one of the most important properties of fats as it influences their functionality in edible and non-edible applications. The physical properties of oils and fats are linked to their saturation degree, to the chain length of the fatty acids they contain and the position of the latter on the glycerol backbone, as well as the symmetry/asymmetry of the fatty acid compositions connected to the glycerol group (De Clercq et al., 2012; Zhang et al., 2009). More precisely, the crystallization, melting behavior and polymorphic stability of fats are determined by the behavior of the triacylglycerols (TAG) they contain. Indeed TAGs, which are the main components of natural oils and fats, organize themselves upon cooling and crystallize into different polymorphic forms depending both on their composition and the processing conditions (Marangoni & Mc Gauley, 2003). This phenomenon is well-known in the industrial production of cosmetics, pharmaceuticals and foods, as it significantly influences the functionality of fat-based products. According to the literature, three basic polymorphs are observed for TAGs, related to the lateral packing of the fatty acid chains; they are called α (hexagonal), β' (orthorhombic), and β (triclinic), in increasing order of melting temperature and stability (Garti & Sato, 2001). For some more complex fats such as cocoa butter (CB), up to six polymorphic forms have however been described (Marangoni & Mc Gauley, 2003).

Mango is one of the most popular fruit crops in Ivory Coast, with an annual production of 180,000 tons (WAAPP/PPAAO, 2017). The local direct consumption and the industrial processing of mango pulp generate high number of seeds which are discarded as waste, while they represent an interesting source of edible fat (Nadeem et al., 2016). According to Solís-Fuentes and del Carmen Durán-de-Bazúa (2020), mango kernel fat (MKF) has significant functional and physicochemical characteristics that makes it possible to replace other fats in food, pharmaceutical or cosmetic industries. MKF is a natural fat containing high amounts of saturated and monounsaturated fatty acids (FA) and is rich in di-saturated TAGs, and more precisely of SUS-type (S = saturated and U = unsaturated), with an oleic acid (O) in sn-2 position (Jin et al., 2021; Van Pee et al., 1981). There is a constant demand for fats rich in di-saturated TAGs (SOS) with a similar composition to CB. Thus, developing processes to produce SOS-rich fats from cheap, reliable and readily available raw materials is of interest (Kadivar et al., 2016). This is what makes MKF interesting for confectionary industries: MKF is indeed one of the six vegetable fats allowed in the manufacture of cocoa butter equivalents (CBEs) (European Union Directive 2000/36/EC, 2000). CBEs are vegetable fats that have physico-chemical properties similar to CB (similar melting profile, composition and polymorphic behavior) and that have been used in confectionery for many years (Sonwai et al., 2021). Solís-Fuentes et al. (2005) investigated the polymorphism of MKF from Manila variety growing in Mexico, using x-ray diffraction. They showed that β was the most prevailing and stable polymorph. On the contrary, Sonwai et al. (2014) showed that β' was the predominant polymorph for MKF var. Kaew (Thailand) solidified at 20°C during 60 min. Some studies reported that MKF chemical composition and thermal behavior is cultivar and origin dependent (Lieb et al., 2019). In this context, we recently extracted MKF from seven specific northern Ivorian varieties with the goal to investigate how such MKF may differ from each other in terms of chemical compositions (Kouassi et al., 2023). It was found

Published in : Journal of the American Oil Chemists' Society (2024), vol. 101, n°1, pp. 67–78
DOI: https://doi.org/10.1002/aocs.12781
Status : Postprint (Author's version)

that the investigated varieties, even if all grown in the same geographic area (North of Ivory Coast, Korhogo state) and collected at the same maturity, were significantly different. Among the seven varieties, four groups were distinguished based on their TAG profile, and more precisely on their StOSt content (St = stearic acid): (1) High-StOSt fat (var. *Djakoumankoun*), (2) Medium-StOSt fat (var. *Dadiani, Brooks*), (3) Low- StOSt fat (var. *Kent, Palmer, Keitt*) and (4) Very low- StOSt fat (var. *Amelie*). The differences found among the four groups are such that their thermal and polymorphic behavior should be different. Based on that, the aim of the work reported here was to investigate the crystallization and polymorphic behavior of three Ivorian MKFs. The three investigated fats were selected based on their chemical composition and their availabilities (one of each of the four proposed groups, except 4 because *Amelie* is not available in sufficient amount for industrial applications).

Materials and methods

SAMPLES

Mango kernel fats (MKF) were extracted from sun-dried mango kernels by maceration at 40°C, using n-hexane as solvent as described by Kouassi et al. (2023) and stored at -20°C until use. Three Ivorian mango varieties, all obtained in Korhogo (North Ivory Coast) were considered: *Kent* (KT), *Brooks* (BR) and *Djakoumankoun* (DN).

FATTY ACID COMPOSITION (FAC)

FAC determination was performed by GC-FID using a Trace GC Ultra gas chromatograph (Thermo Fisher Scientific, Belgium), as described by Mtibaa et al. (2021). FAME were prepared according to AOCS Ce 2–66 method (AOCS, 2009); fatty acids (FA) were identified by comparing their retention times with those of pure standards. The analyses were performed in triplicate and results are expressed as average ± standard deviation.

TRIACYLGLYCEROL PROFILE

TAG analysis was carried out using an HPLC Infinity II 1260 (Agilent Technologies Inc., Santa Clara, CA, USA) system, equipped with a refractive index detector (RID) and a C18 column (RP-18 LiChroCART 250–4.5 µm, 250 mm x 4 mm, Merck, Darmstadt, Germany), both set at a temperature of 30°C, according to IOC method (IOC, 2017). The mobile phase was a mixture of acetone/acetonitrile 57/43 v/v with a flow rate of 1.5 mL/min; injection volume 20 µL. TAGs were determined by their equivalent carbon numbers (ECN) and comparison with known TAGs. The amount of each TAG was expressed in terms of the relative proportion. Two replicates were performed for each sample and data are the average of two independent runs.

Published in : Journal of the American Oil Chemists' Society (2024), vol. 101, n°1, pp. 67–78
DOI: https://doi.org/10.1002/aocs.12781
Status : Postprint (Author's version)

ISOTHERMAL CRYSTALLIZATION BY PULSED NMR

The isothermal crystallization behavior of the MKF was investigated under static conditions at 15 and 20°C (20°C was chosen as it is a common room temperature in Europe and 15°C because 20°C was too high to allow all the samples studied to crystalize under the investigated conditions), using a pulsed Nuclear Magnetic Resonance (p-NMR) spectrometer (Minispec- mq20, Bruker, Karlsruhe, Germany). Calibration was made daily using standards supplied by Bruker (Karlsruhe, Germany) containing 0.0%, 31.3%, and 74.8% of solids. The NMR tubes were filled with liquid MKF. They were put in a dry bath (LAIX, SFC Dry Bath/ PDB6, Germany) set at 80°C for 15 min to ensure a complete erasure of the crystal history and further agitated. The tubes were then transferred in a dry bath (LAIX, SFC Dry Bath/PDB6, Germany) set at the isothermal temperature (15 or 20°C). Once the temperature of the samples reached the crystallization temperature, the tubes were rapidly put into the p-NMR sample port with the temperature set at 15°C or 20°C. Afterwards, SFC measurements were done every 2 min for 2 and 4 h respectively, allowing observation of the crystallization kinetics of the fat samples. All the measurements were performed in triplicate. Mean SFC data were fitted to the Avrami model using non-linear regression (Equation (1)).

$$\frac{SFC(t)}{SFC\infty} = 1 - e^{-Kt^n}, \quad (1)$$

where *SFC (t)* describes the SFC as a function of time, *SFC* ∞ is the limiting SFC as time approaches infinity or reaches equilibrium, *k* is the Avrami rate constant, and *n* is the order of reaction (the Avrami exponent). The constant *k* represents a crystallization rate constant and takes both the nucleation and crystal growth rates into account, whereas the Avrami exponent *n* indicates the crystal growth mechanism (Avrami, 1939).

ISOTHERMAL CRYSTALLIZATION CURVES BY DIFFERENTIAL SCANNING CALORIMETRY (DSC) VIA STOP-AND-RETURN METHOD

The isothermal crystallization behavior of MKF was investigated by DSC using the stop-and-return method as described by Foubert et al. (2008). Samples were analyzed using a Q2000 DSC (TA Instruments, New Castle, DE) calibrated using indium (m.p. 156.6°C) and n-dodecane (m.p. -9.56°C) standards; nitrogen was used as purge gas in order to prevent condensation in the oven. Fat samples (± 4 mg) were hermetically sealed in T0 hermetic pans and an empty pan was used as a reference. The time–temperature program applied was as follows: holding at 80°C for 10 min to ensure the complete fat melting and erase its memory; cooling at -10°C/min to 15 or 20°C; holding for a given specific time (5, 10, 15, 25, 30, 45, 60, 90, 120, 180, 210, 240, 270 and 300 min) at the set isothermal temperature (15°C or 20°C) and further heating at 5°C/min to 80°C (Danthine et al., 2015). For each combination of temperature and time, three replications were performed. The peak temperatures were determined using the Universal Analysis Software version 4.2 (TA Instruments, New Castle, DE).

Published in : Journal of the American Oil Chemists' Society (2024), vol. 101, n°1, pp. 67–78
DOI: https://doi.org/10.1002/aocs.12781
Status : Postprint (Author's version)

ISOTHERMAL CRYSTALLIZATION BY X-RAY DIFFRACTION (XRD)

Polymorphic forms of crystals in the MKFs were determined using a D8 Advance diffractometer (Bruker, Germany) (λ Cu = 1.54178 Å, 40 kV, 30 mA), equipped with a Lynxeye detector (Bruker, Germany) and a temperature control unit (TCU 110 system, Anton Paar, Austria) connected to a water bath (LAUDA, Type PL1 Germany) to control the temperature of the diffractometer chamber TTK 540 (Anton Paar, Graz, Austria). x-Ray measurements were performed in both small (1-15° 2θ) and wide (15-27° 2θ) angles regions, with a 0.02° as step size. Calibration of the peak positions was made using standards: silver behenate, corundum, and with a stabilized β-form of pure tristearin (Lopez et al., 2005). Data was analyzed with the EVA Diffrac.suite software (Bruker, Germany) (Danthine et al., 2019). The applied time–temperature program was the same as for DSC stop and return experiments: holding at 80°C for 10 min to ensure the complete melting of the fat; cooling at -10°C/min to the isothermal crystallization temperature (15 or 20°C) and holding for 5 h at this temperature. Time zero corresponded to the time when the fat reached the desired crystallization temperature. Measurements were performed every 5 min during the isothermal period. As for DSC, an additional measurement was performed after 24 h. All the analyses were conducted in triplicate.

MICROSTRUCTURE

The crystals microstructure of fats crystallized under static condition at 15 or 20°C was observed by Polarized light microscopy (PLM) using a temperature-controlled microscope (Nikon Optical Co., Ltd., Tokyo, Japan), equipped with a digital camera (Sight DS-U3, Nikon Optical Co., Ltd., Tokyo, Japan). Samples were first heated for 10 min at 80°C to destroy all traces of crystal memory, afterwards 20 µL of the molten fat was placed on a pre-tempered glass slide and a pretempered glass cover slip was carefully placed over the sample to produce a uniform thickness. The so-prepared slides were then re-heated in an oven at 80°C for 10 min then placed in a temperature controlled cabinet set at the isothermal crystallization temperature (15 or 20°C). The actual temperature of the material was monitored with a digital thermocouple thermometer (K Type, YC-74UD serial, data logger). Time zero corresponded to the time when the fat reached the desired crystallization temperature. The microstructure was then observed by PLM; a 10x lens was employed to view the microstructures. Images were recorded at defined time points, as for the DSC and XRD experiments. All the analyses were conducted in triplicate.

STATISTICAL ANALYSIS

One-way analysis of variance (ANOVA) and Tukey's test were performed with Minitab 21 software (Minitab Inc., Coventry, U.K.). Statistically significant was defined as $p \leq 0.05$. difference.

Published in : Journal of the American Oil Chemists' Society (2024), vol. 101, n°1, pp. 67–78
DOI: https://doi.org/10.1002/aocs.12781
Status : Postprint (Author's version)

Results and discussion

P-NMR ISOTHERMAL CRYSTALLIZATION

The p-NMR crystallization curves of the three MKFs obtained at 15 and 20°C are presented in Figure 1a,b respectively.

For all MKFs, as expected, the crystallization occurred earlier at 15°C compared to 20°C. The Avrami equation (Equation (1)) was used to characterize the crystallization mechanisms. This equation takes into consideration a nucleation rate and constant linear growth. As it can be seen in Figure 1a, for DN and BR, a large proportion of the fat already crystallized during the cooling, before the temperature reached 15°C. In this case, we only considered the practical application of the simple equation. Different crystallization curves shapes were observed among the three fats and the two temperatures, different shapes mean different crystallization mechanisms. The induction time (tind) was higher at 20°C and the crystallization rate (k) was lower than the one observed at 15°C (Table 2). This is logical and expected as a higher temperature decreases the driving force. Under static condition, if we compare the three fats, at both 15 and 20°C, sample DN crystallized faster as indicated by a higher k, followed by sample BR then KT. It was moreover observed that at 20°C, sample KT was not crystallized after 4 h and that at 15°C, this sample presented the lowest SFC value (30%), this is obviously linked to its lower content of disaturated TAGs and higher content of tri-unsaturated TAGs compared to DN and BR (Table 1). Samples with a different value of n have different crystallization mechanisms. A higher value of n corresponds to a more complex mechanism of crystal growth. As reported by Kawamura (1979) and Rogers et al. (2008), n can range from 0.5 to 4; a n of 4 indicates a spherulitic crystal growth mechanism from sporadic nuclei (nuclei appearing over time), where a n of 3 rep-resents a plate-like or dislike growth mechanism from sporadic nuclei, n of 2 indicates a rod-like growth from sporadic nuclei and $n \leq 1$ is associated to rod-like growth from instantaneous nuclei. The smaller the n value, the faster the nucleation forms and crystals grow (Zhang et al., 2013). The Avrami index n of the three MKF ranged from 1 to 3 with significant differences ($p \leq 0.05$) (Table 2). As a result, depending on the crystallization conditions and on the variety, MKFs presented different crystal morphologies (see Figure 5), the higher n value observed at 15°C for KT indicated sporadic nucleation associated to a disc-like crystal growth, while the relative low n value observed for both BR and DN reflected instantaneous nucleation, with different crystal growth mechanism. The half-time of crystallization (t1/2) is defined as the time during which the crystallization rate is 50% complete. The shorter the half-time was, the faster the crystallization rate obtained. Significant differences were observed between t1/2 with obviously DN having the lowest values, followed by BR and KT.

Regarding the shape of the p-NMR crystallization curves, at 15°C (Figure 1a), a classical one-step crystallization, with a sigmoid shape, was observed for KT, while a non-usual evolution was observed for DN and BR. Indeed, the crystallization curves of both BR and DN are clearly divided into two parts, indicating a particular crystallization process. The unusual SFC decrease at the beginning of the isothermal period (see circled area on Figure 1a) could be due to a melt-mediated polymorphic

Published in : Journal of the American Oil Chemists' Society (2024), vol. 101, n°1, pp. 67–78
DOI: https://doi.org/10.1002/aocs.12781
Status : Postprint (Author's version)

transition from a less stable form into a more stable form (this hypothesis will be discussed later in Section 3.3). Under the investigated conditions, at 20°C (Figure 1b), both BR and DN showed a one-step crystallization. On the contrary, Sonwai and Ponprachanuvut (2014), who studied the static crystallization behavior of MKF from Thai variety Kaew-Morakot using p-NMR, found that this type of MKF (Kaew-Morakot) presented a classical two-step crystallization at 20°C. The difference of crystallization behavior between the two studies could be explained on one hand by different experimental conditions, and mainly by the difference in MKFs chemical composition. Indeed, the Thai Kaew-Morakot MKF is characterized by a lower StOSt (main TAG) content (29%) while BR and DN have higher StOSt contents: 37% and 45%, respectively.

***Table 1**. Fatty acid composition (%total fat means ± SD) and triacylglycerol composition (as average of two replicates) of the three Ivorian mango kernel fats.*

FA	Fatty acid composition		
	BR	DN	KT
C16:0	8.7 ± 0.4[a]	8.3 ± 0.1[a]	9.4 ± 0.0[a]
C18:0	42.5 ± 0.6[a]	48.3 ± 0.0[b]	35.1 ± 0.0[c]
C20:0	2.2 ± 0.2[a]	2.3 ± 0.0[a]	1.8 ± 0.1[b]
SAFA	**53.4 ± 0.8[a]**	**59.0 ± 0.1[b]**	**46.3 ± 0.1[c]**
C18:1n9	41.2 ± 0.7[a]	36.0 ± 0.1[b]	47.0 ± 0.0[c]
C18:2n6	5.2 ± 0.1[a]	4.9 ± 0.0[a]	6.2 ± 0.2[a]
C18:3n3	0.2 ± 0.1[a]	0.3 ± 0.0[a]	0.5 ± 0.1[a]
PUFA	**5.4 ± 0.1[a]**	**5.2 ± 0.0[b]**	**6.7 ± 0.1[c]**
UnSAFA	**46.6 ± 8[a]**	**41.1 ± 0.1[b]**	**53.7 ± 0.1[c]**

Main TAG	Triacylglycerol composition		
OOO	4.8 ± 0.1	2.5 ± 0.0	8.4 ± 0.1
StOP	4.6 ± 0.0	6.0 ± 0.0	3.5 ± 0.1
StLO+OOP	7.5 ± 0.0	5.2 ± 0.0	10.1 ± 0.2
StOO	20.7 ± 0.0	15.5 ± 0.3	25.8 ± 0.2
StLSt	11.7 ± 0.1	12.0 ± 0.1	10.5 ± 0.2
StOSt	37.0 ± 0.0	45.8 ± 0.6	26.3 ± 0.4

Note: Significant differences of means ($p \leq 0.05$) within a row are indicated by different letters.

Abbreviations: KT, Kent; DN, Djakoumankoun; BR, Brooks; PUFA, polyunsaturated fatty acid; SAFA, saturated fatty acid; UnSAFA, unsaturated fatty acid.

Published in : Journal of the American Oil Chemists' Society (2024), vol. 101, n°1, pp. 67–78
DOI: https://doi.org/10.1002/aocs.12781
Status : Postprint (Author's version)

***Table 2**. Avrami kinetic parameters (as average of three replicates) of isothermal crystallization curves at 15 and 20°C for the three mango kernel fat varieties; KT, BR and DN.*

Parameter sample	15°C (2 h)				20°C (4 h)		
	$K*10^{-4}$ (min)	n	t_i (min)	$t_{1/2}$ (min)	$K*10^{-4}$ (min)	n	t_i (min)
BR	200 ± 0.01	1.6 ± 0.03	Prior Tc	12.6 ± 1.12	20 ± 0.00	1.8 ± 0.07	103 ± 2.
DN	2000 ± 0.01	0.9 ± 0.01	Prior Tc	4.2 ± 0.2	800 ± 0.03	1 ± 0.12	54.5 ± 1
KT	1.1 ± 0.00	2.7 ± 0.2	41.5 ± 0.1	23.7 ± 1.36	–	–	–

Abbreviations: BR, Brooks; DN, Djakoumankoun; KT, Kent; Tc, crystallization temperature.

***Figure 1**. pNMR isothermal crystallization curves obtained at 15°C (a) and 20°C (b) for the three mango kernel fat; Djakoumankoun (DN), Brooks (BR) and Kent (KT).*

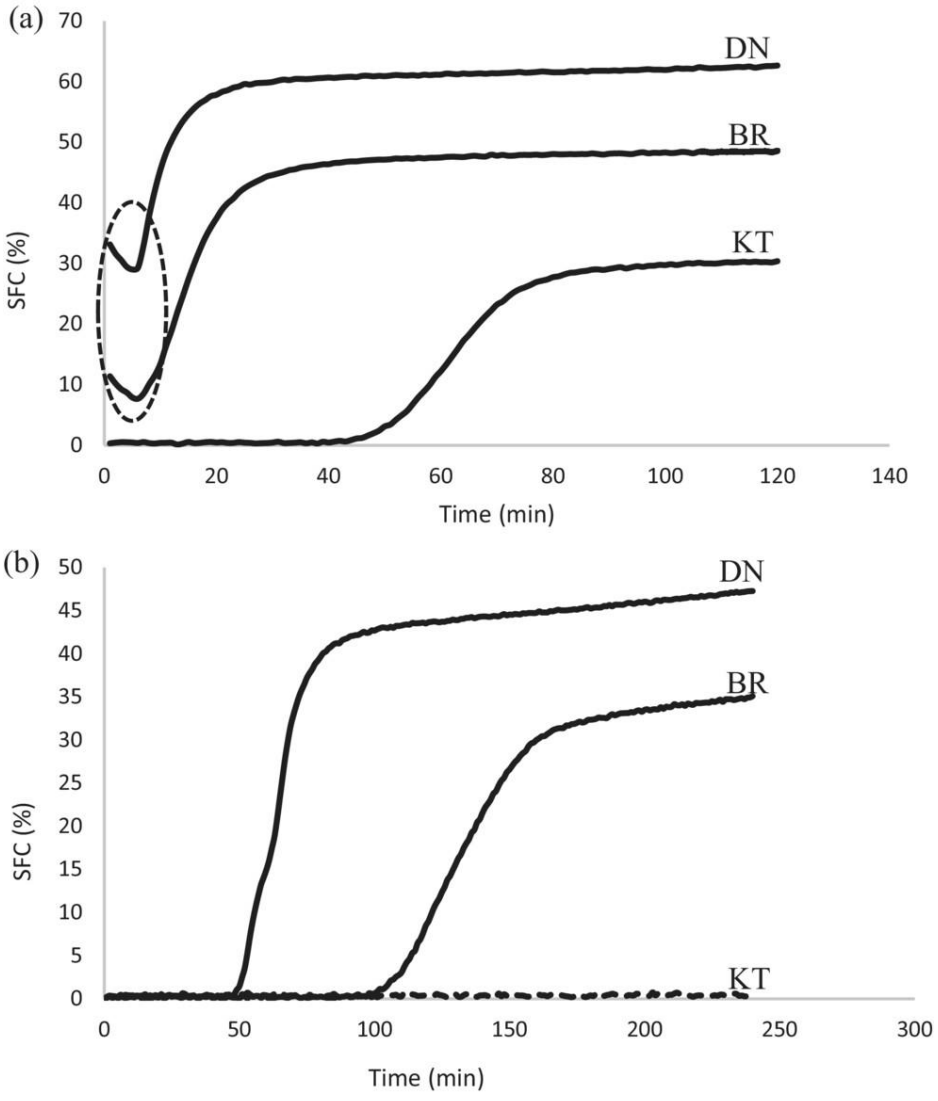

Published in : Journal of the American Oil Chemists' Society (2024), vol. 101, n°1, pp. 67–78
DOI: https://doi.org/10.1002/aocs.12781
Status : Postprint (Author's version)

DSC ISOTHERMAL CRYSTALLIZATION (STOP & RETURN EXPERIMENTS)

To better characterize the isothermal crystallization behavior of the three investigated MKF, DSC stop & return experiments were conducted as described by Foubert et al. (2008). Indeed, in DSC stop and return experiments, the melting profiles are recorded after different isothermal crystallization times and are used to monitor the degree of crystallization. By this way this method allows to monitor the crystallization extent as a function of time, even if some crystallization already occurred before reaching the isothermal temperature, which was observed by p-NMR for DN and BR at 15°C (see Section 3.1).

Results obtained are presented in Figure 2a–c and in Figure 2d-f for 15°C and 20°C, respectively. At 15°C, as can be observed in Figure 2a,b for BR and DN, at the early stage of the isothermal period, a first low melting peak at about 18 and 19°C, respectively, occurred which rapidly tended to decrease in area and finally disappeared in favor of a higher melting peak (medium melting peak) at about 27-32°C. From this it can be hypothesized that a polymorphism transition from a less stable to a more stable polymorph took place. This higher melting peak continued to grow even after disappearance of the first peak, indicating an increasing amount of crystallized material. Afterwards, a shoulder was observed at the right side of this peak (5 h), which in turn, grew and resulted in a higher melting peak located at 35-36°C after 24 h of isothermal time.

The study of Solís-Fuentes et al. (2005) aimed at studying the predominant polymorphic forms of MKF from Manila variety (Mexico) by DSC and x-ray diffraction. They observed different crystalline forms: α, β' and β and reported their corresponding melting temperature α:18.5°C, β': 29.4°C, mixed polymorphs: 35.2°C and β: 40°C. Sagiri et al. (2014) reported the existence of five polymorphic forms for MKF from India and their melting point: viz sub-α or γ: 11.1°C, α: 19.9°C, β'_2: 25.5°C, β'_1: 29.6°C and β-form: 38°C. Sonwai et al. (2021) also reported a melting point of 28-29°C for β'_1 and 33°C for the mix of β'_1 and β polymorphs. In this case, for DN and BR, the evolution of the DSC melting peaks as a function of the duration of the isothermal period (Figure 2) suggests the formation of α polymorph from the melt in the first stage of crystallization, followed by polymorphic transitions where the already formed α-crystals convert into more stable β' and β forms. For sample BR (Figure 2a), the first lower melting peak that appeared at around 18°C should correspond to the melting of the α-form; the second observed at around 28°C is consistent with the β'_2-form while the last higher melting peak observed at about 36°C should correspond to β-form. For sample DN (Figure 2b), the first melting peak was observed at about 19°C and corresponded to α-form, the second endothermal event made of two sub-peaks at around 28°C and 31°C is probably indicative of a mix of β' polymorphs (β'_2 and β'_1, respectively); and the last high melting peak observed at about 36°C after 24 h of static crystallization corresponded to the melting of a β-stable form. The melting curve obtained for KT (Figure 1c) suggests that the initial crystallization occurred directly from the melt into β'-crystal, which further transformed into β-stable polymorph over the time. Indeed, the first occurring peak was detected after 25 min of isothermal period and it was located at about 27°C (β'_2), the second one was observed at about 33°C and is attributed to β-stable form (Figure 2c).

At 20°C, no crystallization was observed for KT during the 5 h of isothermal period; a sharp peak at about 35°C was however observed after 24 h at 20°C, corresponding to the melting of a β-stable

Published in : Journal of the American Oil Chemists' Society (2024), vol. 101, n°1, pp. 67–78
DOI: https://doi.org/10.1002/aocs.12781
Status : Postprint (Author's version)

polymorph. For samples BR and DN a broad peak was already detected at the beginning of the crystallization (melting peak around 32°C), coinciding with the presence of the β'_1 polymorph. This broad peak then grew indicating an increasing amount of crystals, afterwards a sharp higher melting peak at about 35°C (β) was present for BR (Figure 2d) while in the same time a high melting region made of two sub-peaks (melting peak at about 33 and 36°C) was observed for DN (Figure 2e), corresponding to a crystal mix of β'_2 and β.

***Figure 2**. Differential scanning calorimetry stop and return crystallization curves obtained at 15°C (a-c) and 20°C (d-f) for mango kernel fat samples BR [a and d], DN [b and e] and KT [c and f]. Each curve corresponds to the melting thermograms after isothermal crystallization for different periods of time.*

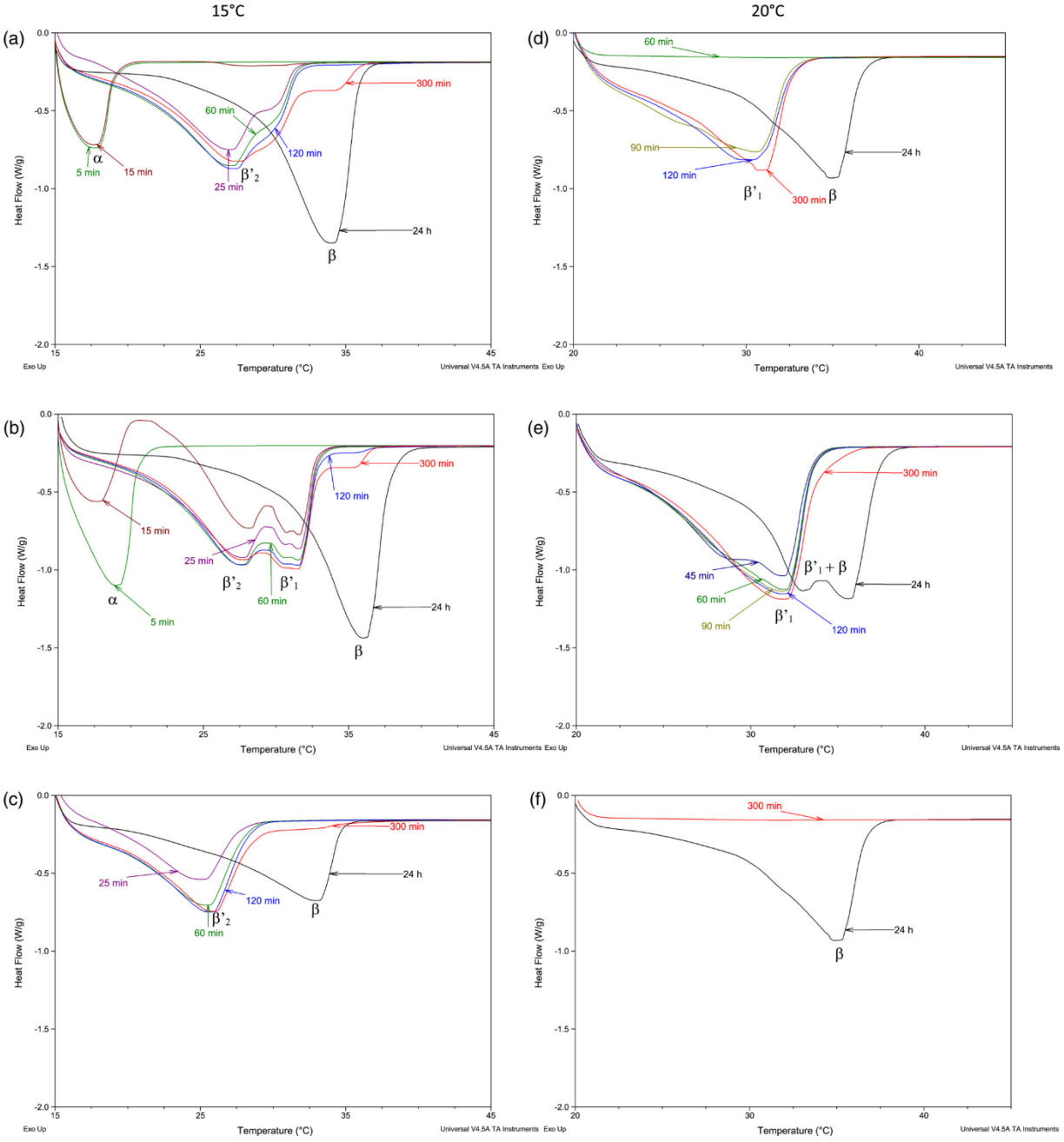

Published in : Journal of the American Oil Chemists' Society (2024), vol. 101, n°1, pp. 67–78
DOI: https://doi.org/10.1002/aocs.12781
Status : Postprint (Author's version)

ISOTHERMAL CRYSTALLIZATION BY X-RAY DIFFRACTION (XRD)

To verify all the hypotheses regarding the polymorphic behavior based on the DSC curves (see Section 3.2), isothermal XRD experiments were conducted in the same conditions as for the DSC stop-and-return experiment (same cooling rate, same isothermal temperature, same duration) to monitor the polymorphism of the MKF during the isothermal period. All the polymorphic forms observed in this study and their thermal characteristics are listed in Table 3.

Figures 3 and 4 present the XRD data obtained at 15°C and 20°C respectively, as a function of time. At 15°C, for both BR and DN samples, the first crystallization step was characterized by the presence of a diffraction peak corresponding to a distance of about 4.15 Å in the short spacings region and a long spacing of 55 Å (Figure 3a,b). This corresponded to the unstable α polymorph in a double chain length conformation. For BR, this α-2L form was further (after 15 min) converted to β'-3L form, with short spacing at *d* = 4.28 Å, 4.15 Å and 3.86 Å and long spacing at *d* = 70 Å (Figure 3a), while for DN, the α-2 L was transformed into β'-3L with short spacing at *d* = 4.55 Å, 4.44 Å, 4.28 Å, 4.13 Å, 3.86 Å and long spacing = 70 Å (Figure 3b). At the end of the isothermal period (24 h), both BR and DN were crystallized into β-3L with short spacing observed at *d* = 5.43 Å, 4.59 Å, 4.00 Å, 3.88 Å, 3.77 Å, 3.67 Å and long spacing at *d* = 65 Å. In contrast to BR and DN, the sample KT crystallized directly from liquid state to β'-3L (short spacing at *d* = 3.86 Å, 4.13 Å, 4.28 Å and long spacing at *d* = 70 Å, similar to BR) without passing through the α-form, then it evolved into the stable β-3L form (short spacing at *d* = 5.43 Å, 4.59 Å, 4.00 Å, 3.88 Å, 3.77 Å, 3.67 Å and long spacing at *d* = 65 Å) (Figure 3C). At 20°C, as previously mentioned, KT did not crystallize during the isothermal period of 5 h, contrarily to BR and DN. For these two fats, the initial peaks observed at 20°C in the wide-angle region corresponded to an interplanar distance (short spacing) of 4.15 Å and 3.86 Å, which means β' polymorph. Interestingly, both bilayer (2L, *d* = 45.4 Å) and tri-layer stacking were observed for BR (3L, *d* = 70 Å), while for DN only a trilayer (3L = 70 Å) was observed. These peaks grew over time, both in the long and the short spacing regions, indicating an increase in the amount of the β' polymorphs. After 24 h of isothermal period at 20°C, β-3L stable polymorph with some traces of β'-3L (short spacing at *d* = 5.43 Å, 4.59 Å, ((4.20 Å)), 4.00Å, 3.88 Å, 3.77 Å, 3.67 Å and long spacing at *d* = 65 Å (and 70 Å)) were present in BR, while for DN a blend of β'-3L + β-3L was clearly observed (short spacing at *d* = 5.43 Å, 4.59 Å, 4.18 Å, 4.00 Å, 3.86 Å, 3.77 Å, 3.67 Å and long spacing at *d* = 70 and 65 Å). As can be noticed, the polymorphic transition from β' to β stable form was delayed for DN compared to BR. This was clearly visible in both short spacings and long spacings data where the ratio between the peak at *d* = 65 Å (*n* = 2)/peak at *d* = 70 Å (*n* = 2) is higher for BR compared to DN.

The three investigated MKF were β-stable fat, like cocoa butter. Moreover, as can be seen in Figure 4a on the left, after 24 h of static isothermal crystallization, the x-ray diffraction pattern (short spacing) of BR is very similar to that of the β_2 (V) phase (5.43, 4.59, 3.98, 3.86, 3.75 and 3.66 Å) ofCB as reported by Silva et al. (2009), suggesting that the fat seems to be quite stable in β_2-form.

Moreover, the XRD data allowed to explain the unusual shape observed in the crystallization curve obtained by p-NMR (Section 3.1.—Figure 1): for sample BR and DN, the observed particular evolution associated to the decrease in SFC at the beginning of the isothermal crystallization at 15°C corresponded to a melt-mediated polymorphic transition from α-form to β'-form. This transition is

Published in : Journal of the American Oil Chemists' Society (2024), vol. 101, n°1, pp. 67–78
DOI: https://doi.org/10.1002/aocs.12781
Status : Postprint (Author's version)

evident in the DSC curve where a crystallization peak is clearly observed for DN (Figure 2b). Subsequently, a solid–solid transition resulted in the formation of stable β-crystals. This behavior of α-melt mediation had not been reported yet in the literature for MKF.

Figure 3. *(a–f) X-ray diffraction pattern of three mango kernel fat samples; BR [AD], DN [BE] and KT [CF] crystallized isothermally for 24 h (1440 min). Left column corresponds to the long spacings and the right column corresponds to the short spacings.*

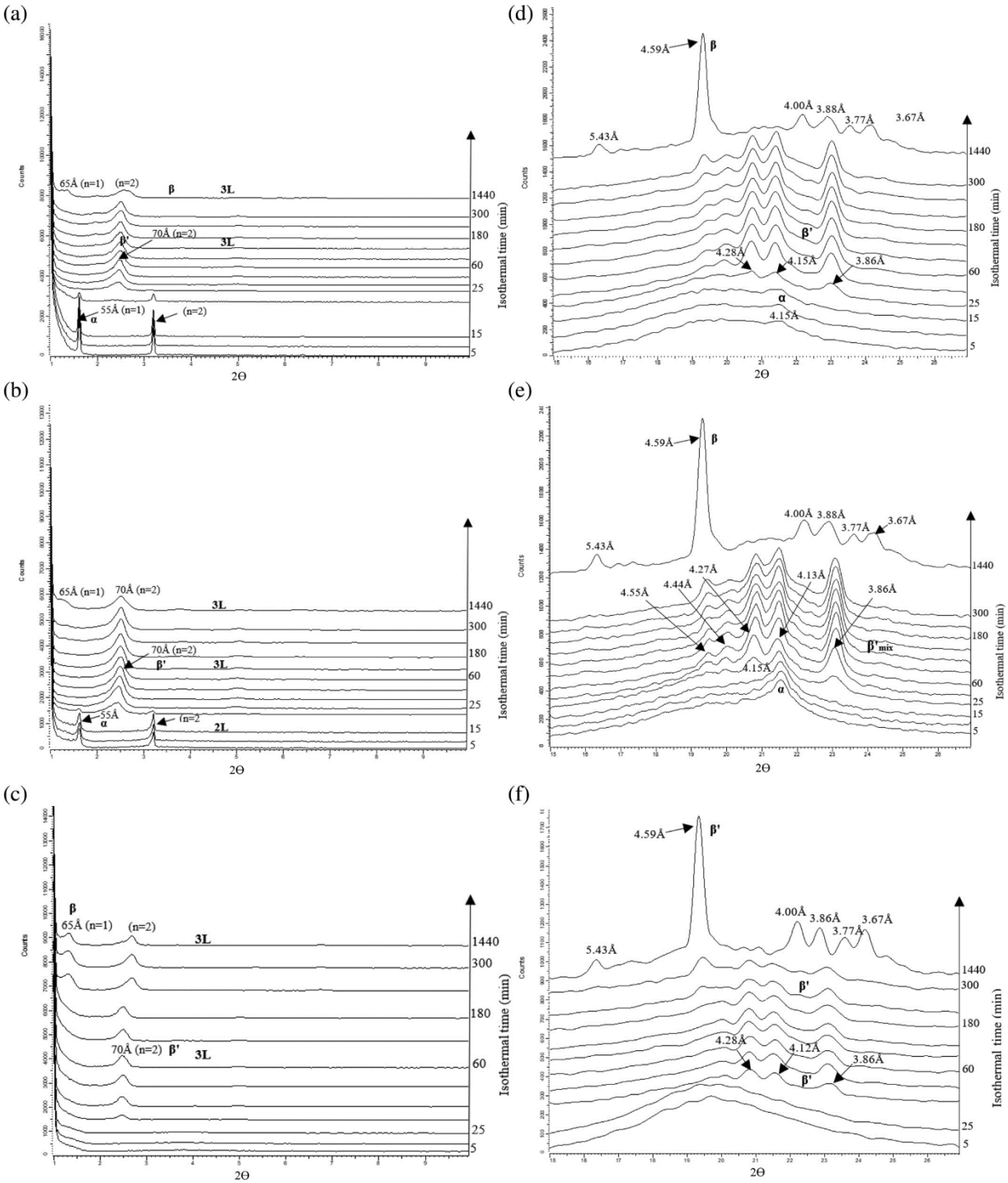

Published in : Journal of the American Oil Chemists' Society (2024), vol. 101, n°1, pp. 67–78
DOI: https://doi.org/10.1002/aocs.12781
Status : Postprint (Author's version)

***Figure 4**. X-ray diffraction pattern of the three mango kernel fat samples: BR [a] and DN [b] crystallized isothermally at 20°C for 24 h (1440 min). Left column corresponds to the long spacings region and the right column corresponds to the short spacings region.*

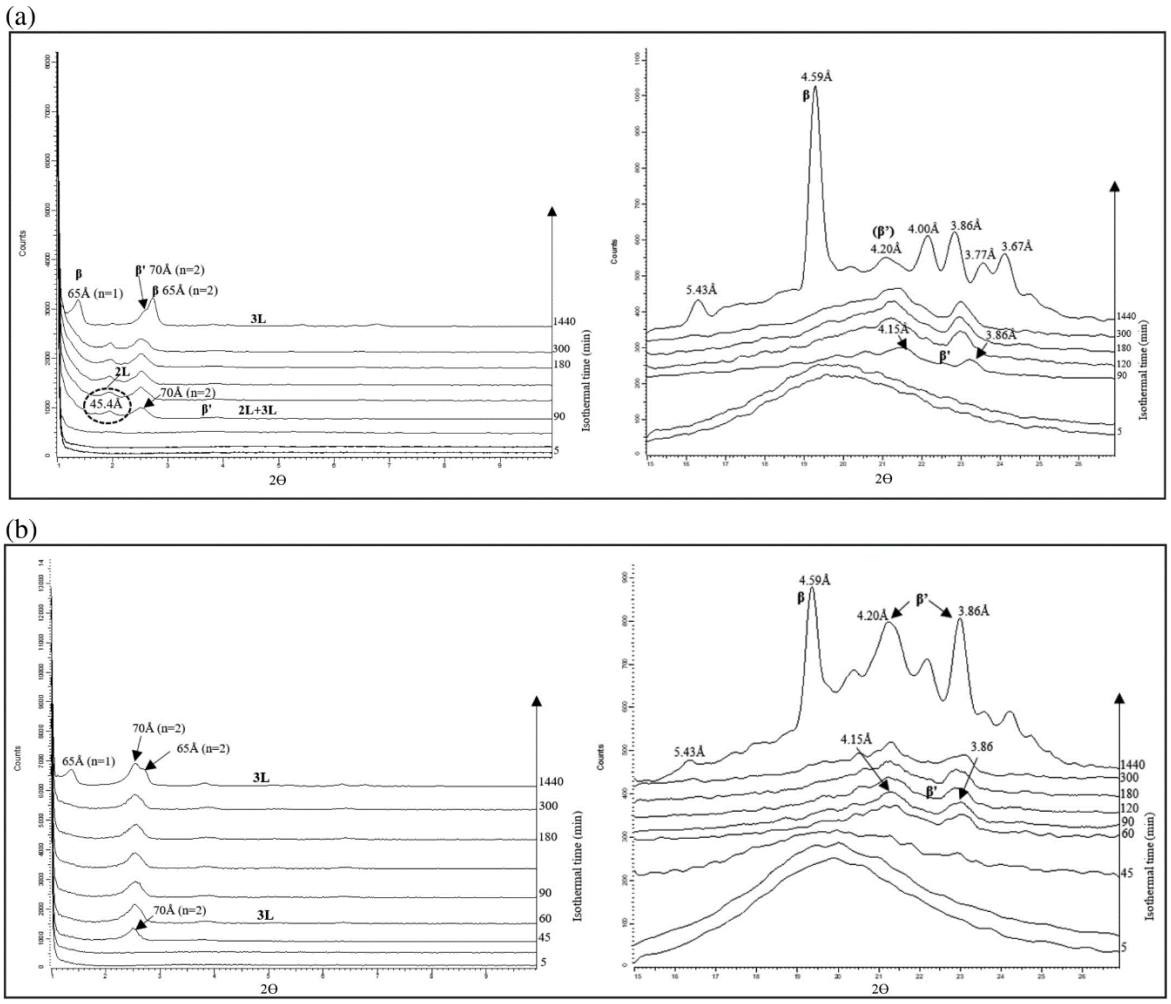

***Table 3**. Characteristics of polymorphic forms and thermal properties of Ivorian mango kernel fat obtained from DSC-XRD data.*

Polymorphic phases	Short spacing (Å)	Long spacing (Å)	Melt temperature (°C)
α	4.15	55 (2L)	18–19
β'_2	4.28, 4.15, 3.86	71 (3L)	27–29
	4.28, 4.13, 3.86	70 (3L)	
	4.15, 3.86	71 (2L)	
β'_1	4.55, 4.44, 4.28, 4.13, 4.86	70 (3L)	30–33
Mixed (β' + β)	5.43, 4.59, 4.18, 4.00, 3.86, 3.77, 3.67	70, 65 (3L)	
β	5.43, 4.59, 4.00, 3.88, 3.77, 3.66	66 (3L)	35–36

Published in : Journal of the American Oil Chemists' Society (2024), vol. 101, n°1, pp. 67–78
DOI: https://doi.org/10.1002/aocs.12781
Status : Postprint (Author's version)

MICROSTRUCTURE

Crystalline microstructure was investigated at 15°C and 20°C, using polarized light microscopy (PLM). Figure 5a shows the microstructure of fat crystals formed at 15°C. After 5 min of crystallization, a large number of crystallites was observed for all MKFs, except for KT which was still liquid. Crystal morphology observed for BR and DN can be described as made of a high number of very small needle-shaped crystallites, corresponding to α polymorph as evidenced by XRD analysis (Figure 3a,b), this is similar to the observation made by Marangoni and Mc Gauley (2003) for the α-form of cocoa butter. Over the first hours of crystallization, the microstructure was relatively comparable for samples BR and DN, but again not for KT. The latter showed a fewer number of small disk-shaped crystals surrounded by substantial proportions of liquid phase compared to the others, this is logical regarding the FA composition of the three samples (see Table 1). Figure 5b. shows the microstructure of the three MKF crystallized at 20°C. After 90 min, DN and BR crystals were of urchin shaped type, surrounded by substantial proportion of liquid phase, which was obviously higher for BR. Over time, the solid fraction increased, as reflected in the increase in the number of crystals as well as the size of the existing crystals. Regarding sample KT where no crystallization was observed after 5 h, after 24 h at 20°C a microstructure made of disk-shaped fat crystals, with a smooth and shiny appearance, but with a high proportion of liquid phase was observed.

***Figure 5**. Polarized light micrograph of three mango kernel fat varieties crystallized isothermally at 15°C (a) and 20°C (b).*

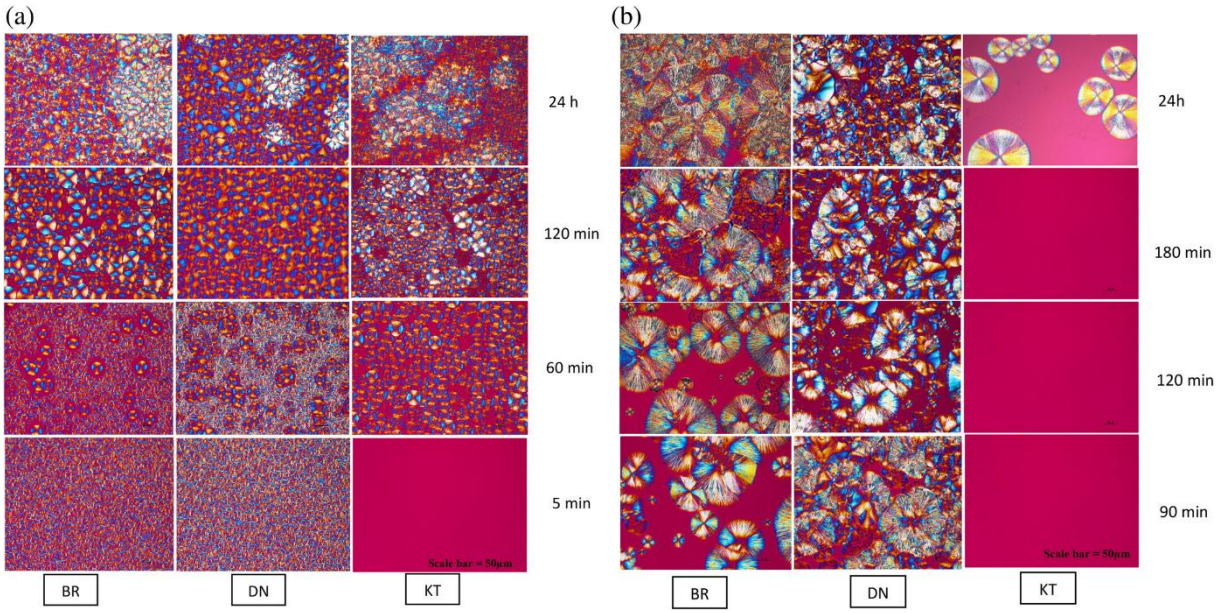

Published in : Journal of the American Oil Chemists' Society (2024), vol. 101, n°1, pp. 67–78
DOI: https://doi.org/10.1002/aocs.12781
Status : Postprint (Author's version)

RELATION BETWEEN CRYSTALLIZATION BEHAVIOR AND TAG COMPOSITION

The three MKF studied showed different crystallization behavior. This is obviously linked to their different TAG composition. Indeed, as mentioned in the introduction section, the three investigated MKF were selected based on the classification we previously made: DN is a High-StOSt fat, BR is a Medium-StOSt fat, and KT is a Low-StOSt fat (Kouassi et al., 2023). For the three selected fats, the main TAG were StOSt, StOO, and StLSt (with St = stearic acid, O = oleic acid, and L = linoleic acid) but in different proportions (Table 1). The structural properties of these pure TAG are reported in literature: StOSt presents five polymorphic forms (α-2L, γ-3L, β'-3L, β_2-3L and β_1-3L), StOO three (sub-α-2L, α-3L, and β'-3L) (Ueno et Sato, 1999; Timms, 1984; Zhang et al., 2009) while for StLSt only two forms are reported (α-2L and γ-3L) (Takeuchi et al., 2002) (Table 4). Takeuchi et al. (2002) also reported that specific interactions between StOSt and StLSt existed. According to Ueno et al. (1999), StOSt in both β' and β-forms crystallize in 3L-type structure, with long spacings at around 70 and 65 Å, respec-tively. Indeed, for symmetrical unsaturated TAGs such as POP or StOSt and in mixtures with high SatOSat content, the polymorphic β-3L form is preferred to allow the unsaturated chain to separate from the two saturated ones. On the contrary, due to the two unsaturated chains, StOO will prefer to pack in β' structure as this is less compact (Sato, 2018; Timms, 1984).

At 20°C, for BR, interestingly the presence of both 2L and 3L structures was observed for β'-crystals, it may indicate a particular interaction, such as the forma-tion of a molecular compound (2L). According to Sato and Ueno (2001) the transformation into a molecular compound crystal for the mixture of unsaturated-saturated mixed acid TAGs occurs in 2L structure, as a result of steric hindrance. On the other hand, the molecular interactions observed for sample DN play a different role: only 3L stacking was observed for both β' and β crystals. Moreover, the kinetics of polymorphic transformation were different in both fats, especially regarding the polymorphic transition from β' to β stable form, which was delayed for DN compared to BR. This may be interpreted by considering their liquid fractions. The StOO, POO/StLO and OOO contents are higher in sample BR compared to DN (Table 1). Higher content of low melting TAGs increases the TAGs mobility and facilitates polymorphic transitions. Thus, a higher amount of liquid in BR allows TAGs to rearrange themselves more easily into the fat crystal network, leading to more stable polymorphic forms (Danthine et al., 2015). At 15°C, the behavior of DN and BR was more similar, as less liquid oil was present at that temperature compared to 20°C, as can be seen in the microstructure (Figure 5a,b).

Published in : Journal of the American Oil Chemists' Society (2024), vol. 101, n°1, pp. 67–78
DOI: https://doi.org/10.1002/aocs.12781
Status : Postprint (Author's version)

***Table 4**. Polymorphic forms of StOSt, StOO and StLSt (ref. Timms (1984), Ueno et al. (1999), and Zhang et al. (2009)).*

Triacylglycerol	Long spacing (Å)	Short spacing (Å)
StOSt		
α	48; 56	4.1; 4.2
γ	71; 74	4.7; 3.9
β'	70	4.24; 3.9; 4.30; 4.15; 4.02; 3.95; 3.83; 3.70
β_2	65	4.58; 4.0; 3.9; 3.67; 3.57;
β_1	65	4.6; 4.58; 4.02; 3.97; 3.85; 3.80; 3.65
StOO		
α	60	4.2
β'	67.4; 66	4.4; 4.3; 4.0; 3.9;
β		
StLSt		
α	54	
γ	73	4.5; 3.85

Conclusions

In this work, the crystallization and polymorphic behaviors of three Ivorian MKF were investigated. The polymorphic phases detected for the MKF were identified as α, β'_2, β'_1 and β. Due to their high StOSt content, the three investigated samples are β-3L tending. However, the data from DSC, p-NMR, PLM and XRD experiments revealed that different behaviors/ kinetics existed among the three MKFs, resulting from different triacylglycerol composition, especially the main ones: StOSt, StOO, StLSt, POO/StLO and OOO. DN always crystallized faster compared to the other samples; however, at 20°C the polymorphic transition from β' to β was delayed for DN compared to BR. These different behaviors result from the interaction between the main TAG during crystallization that dictates the crystallization rate and polymorphic transformations. On one hand, StOO, POO/StLO and OOO could act as solvent (liquid oil), increasing the mobility of TAGs, which promoted some rearrangements within the fat crystal network. On the other hand, StOO could have an impact on StOSt crystallization, and its effect depends on the temperature and their ratio (StOO/ StOSt), which corresponded to 0.3, 0.6, and 1 for DN, BR and KT, respectively. Finally, the results of this study are useful for the fat industry as they could help to develop new fat-based products based on Ivorian MKF. However, special care should be taken if CBEs are to be made, as compositions and polymorphic behavior differ among the varieties.

Published in : Journal of the American Oil Chemists' Society (2024), vol. 101, n°1, pp. 67–78
DOI: https://doi.org/10.1002/aocs.12781
Status : Postprint (Author's version)

AUTHOR CONTRIBUTIONS

Sabine Danthine and Alfred Kouakou Kouassi conceived and designed the study; Alfred Kouakou Kouassi wrote the first draft of the manuscript; Sabine Danthine proofread the manuscript; Alfred Kouakou Kouassi carried out the research; Giorgia Purcaro and Erica Moret performed the chromatography analysis and analyzed chromatography data; Taofic Alabi and Sabine Danthine supervised the study. Christophe Blecker provided financial and material support. All authors contributed to and approved the final draft of the manuscript.

ACKNOWLEDGMENTS

The authors acknowledge financial support from the government of the Ivory Coast and the university of Liège (Belgium). We also wish to acknowledge the laboratory of Food Science and Formulation (University of Liège-Gembloux Agro-Bio Tech, Belgium) for material support. The authors are grateful to Lynn Doran and Filocco Sandrino for their skilful technical assistance. The authors would like to thank again Lynn Doran for proofreading and editing this manuscript in English.

Published in : Journal of the American Oil Chemists' Society (2024), vol. 101, n°1, pp. 67–78
DOI: https://doi.org/10.1002/aocs.12781
Status : Postprint (Author's version)

References

AOCS Methods. Official methods and recommended practices of the AOCS. 6th ed. Urbana, Ill: AOCS; 2009.

Avrami M. Kinetics of phase change. I general theory. J Chem Phys. 1939;7(12):1103–12.

Danthine S, Delatte S, Blecker C, Smith KW, Bhaggan K. Crystallization behaviour of binary fat blends containing shea stearin as hard fat. Eur J Lipid Sci Technol. 2015;117(11):1687–99.

Danthine S, Vors C, Agopian D, Durand A, Guyon R, Carrière F, et al. Homogeneous triacylglycerol tracers have an impact on the thermal and structural properties of dietary fat and its lipolysis rate under simulated physiological conditions. Chem Phys Lipids. 2019;225:104815.

De Clercq N, Danthine S, Nguyen MT, Gibon V, Dewettinck K. Enzymatic interesterification of palm oil and fractions: monitoring the degree of interesterification using different methods. J Am Oil Chem Soc. 2012;89(2):219–29.

Foubert I, Fredrick E, Vereecken J, Sichien M, Dewettinck K. Stopand-return DSC method to study fat crystallization. Thermochim Acta. 2008;471(1–2):7–13.

Garti N, Sato K, editors. Crystallization processes in fats and lipid systems. Boca Raton: CRC Press; 2001.

International Olive Council (IOC). COI/T.20/Doc. No 30 /Rev. 2 Determination of the difference between actual and theoretical content of triacylglycerols with ECN 42. 2017.

Jin J, Jin Q, Akoh CC, Wang X. StOSt-rich fats in the manufacture of heat-stable chocolates and their potential impacts on fat bloom behaviors. Trends Food Sci Technol. 2021;118:418–30.

Kadivar S, De Clercq N, Danthine S, Dewettinck K. Crystallization and polymorphic behavior of enzymatically produced sunflower oil based cocoa butter equivalents. Eur J Lipid Sci Technol. 2016;118(10):1521–38.

Kawamura K. The DSC thermal analysis of crystallization behavior in palm oil. J Am Oil Chem Soc. 1979;56(8):753–8.

Kouassi KA, Alabi T, Purcaro G, Cissé M, Moret S, Moret E, et al. (in press). Assessment of composition, color and oxidative stability of mango (Mangifera indica L) kernel fats from various Ivorian varieties. J Am Oil Chem Soc. 2023. https://doi.org/10.1002/aocs.12758

Lieb VM, Schuster LK, Kronmüller A, Schmarr HG, Carle R, Steingass CB. Fatty acids, triacylglycerols, and thermal behaviour of various mango (Mangifera indica L.) kernel fats. Food Res Int. 2019;116:527–37.

Lopez C, Lesieur P, Bourgaux C, Ollivon M. Thermal and structural behavior of anhydrous milk fat. 3. Influence of cooling rate. J Dairy Sci. 2005;88(2):511–26.

Marangoni AG, Mc Gauley S. Relationship between crystallization behaviour and structure in cocoa butter. Cryst Growth Des. 2003;3(1):95–108.

Mtibaa I, Zouari A, Attia H, Ayadi MA, Danthine S. Effects of physical ripening conditions and churning temperature on the buttermaking process and the physical characteristics of camel milk butter. Food Bioproc Tech. 2021;14(8):1518–28.

Nadeem M, Imran M, Khalique A. Promising features of mango (Mangifera indica L.) kernel oil: a review. J Food Sci Technol. 2016; 53:2185–95.

Published in : Journal of the American Oil Chemists' Society (2024), vol. 101, n°1, pp. 67–78
DOI: https://doi.org/10.1002/aocs.12781
Status : Postprint (Author's version)

Official Journal of the European Communities. Directive of 23 June 2000 relating to cocoa and chocolate products intended for human consumption. Directive 2000/36/EC, 19, L197. 2000.

Rogers MA, Tang D, Ahmadi L, Marangoni, AG. Fat crystal networks. In: Aguilera JM, Lillford PJ, editors. Food Materials Science. New York, NY: Springer; 2008. https://doi.org/10.1007/978-0-387-71947-4_17

Sagiri SS, Sharma V, Basak P, Pal K. Mango butter emulsion gels as cocoa butter equivalents: physical, thermal, and mechanical analyses. J Agric Food Chem. 2014;62(47):11357–68.

Sato K. Polymorphism of lipid crystals. Crystallization of lipids. In: Fundamentals and applications in food, cosmetics, and pharmaceuticals. Hoboken, New Jersey: John Wiley & Sons Ltd.; 2018. p. 17–60. https://doi.org/10.1002/9781118593882.ch2

Sato K, Ueno S. Molecular interactions and phase behavior of polymorphic fats. Crystallization processes in fats and lipid systems. Boca Raton: CRC Press; 2001. p. 191–224.

Silva JC, Plivelic TS, Herrera ML, Ruscheinsky N, Kieckbusch TG, Luccas V, et al. Polymorphic phases of natural fat from Cupuassu (Theobroma grandiflorum) beans: a WAXS/SAXS/DSC study. Cryst Growth des. 2009;9(12):5155–63.

Solís-Fuentes JA, del Carmen Durán-de-Bazúa M. Mango seed: mango (Mangifera indica L.) seed and its fats. Nuts and seeds in health and disease prevention. Cambridge, MA: Academic Press; 2020. p. 79–90.

Solís-Fuentes JA, del Rosario Hernández-Medel M, del Carmen Durán-de-Bazúa M. Determination of the predominant polymorphic form of mango (Mangifera indica) almond fat by differential scanning calorimetry and X-ray diffraction. Eur J Lipid Sci Technol. 2005;107(6):395–401.

Sonwai S, Kaphueakngam P, Flood A. Blending of mango kernel fat and palm oil mid-fraction to obtain cocoa butter equivalent. J Food Sci Technol. 2014;51:2357–69.

Sonwai S, Ornla-ied P, Martini S, Hondoh H, Ueno S. High-intensity ultrasound-induced crystallization of mango kernel fat. J Am Oil Chem Soc. 2021;98(1):43–52.

Sonwai S, Ponprachanuvut P. Studies of fatty acid composition, physicochemical and thermal properties, and crystallization behavior of mango kernel fats from various Thai varieties. J Oleo Sci. 2014;63(7):661–9.

Takeuchi M, Ueno S, Flöter E, Sato K. Binary phase behavior of 1, 3-distearoyl-2-oleoyl-sn-glycerol (SOS) and 1, 3-distearoyl-2-linoleoyl-sn-glycerol (SLS). J Am Oil Chem Soc. 2002;79: 627–32.

Timms RE. Phase behaviour of fats and their mixtures. Prog Lipid Res. 1984;23(1):1–38.

Ueno S, Minato A, Yano J, Sato K. Synchrotron radiation X-ray diffraction study of polymorphic crystallization of SOS from liquid phase. J Cryst Growth. 1999;198:1326–9.

Van Pee WM, Boni LE, Foma MN, Hendrikx A. Fatty acid composition and characteristics of the kernel fat of different mango (Mangifera indica) varieties. J Sci Food Agric. 1981;32(5): 485–8.

WAAPP/PPAAO. (2017), http://www.waapp-ppaao.org/cotedivoire

Zhang L, Ueno S, Sato K, Adlof R, List G. Thermal and structural properties of binary mixtures of 1, 3-distearoyl-2-oleoyl-glycerol (SOS) and 1, 2-dioleoyl-3-stearoyl-sn-glycerol (sn-OOS). J Thermal Anal Calorim. 2009;98(1):105–11.

Zhang X, Li L, Xie H, Liang Z, Su J, Liu G, et al. Comparative analysis of thermal behavior, isothermal crystallization kinetics and polymorphism of palm oil fractions. Molecules. 2013;18(1): 1036–52.